Effect of solid particle size on the viscosity of a secondary copper smelting slag

Olivier Vergote[1], Inge Bellemans[2], Kim Verbeken[3], Amy Van den Bulck[4]

1. Postdoctoral researcher, Ghent University, Department of Materials, Textiles and Chemical Engineering, Gent (Belgium), 9052. Olivier.vergote@ugent.be
2. Assistant professor, Ghent University, Department of Materials, Textiles and Chemical Engineering, Gent (Belgium), 9052. Inge.bellemans@ugent.be
3. Associate professor, Ghent University, Department of Materials, Textiles and Chemical Engineering, Gent (Belgium), 9052. Kim.verbeken@ugent.be
4. R&D competence manager, Umicore N.V., Umicore Research & Development, Olen (Belgium), 2250. Amy.VandenBulck@eu.umicore.com

Keywords: Pyrometallurgy, copper smelting, slag chemistry, slag viscosity, spinel, experimental measurements, physico-chemical properties

ABSTRACT

Viscosity is one of the most important physicochemical properties during pyrometallurgical operations. In the sub-liquidus regime, an important factor is the presence of suspended solid particles, yet its influence is not well-described in earlier literature, despite the significance of this factor. This project aims to determine the influence of spinel particles ($Zn(Al,Fe)_2O_4$) on the rheology of a multiphase synthetic PbO-SiO_2-ZnO-Fe_2O_3-CaO-Al_2O_3 slag system. Three datasets with a well-controlled methodology and three different spinel sizes (small (13 µm), medium (34 µm) and large particles (76 µm)) were published previously, using a custom-built high-temperature rheometer. This study presents an additional dataset of slag viscosity measurements, performed using a different apparatus, the Anton Paar FRS 1800, to verify the consistency of the earlier determined viscosity behaviour. Within this dataset, no consistent trend could be found between the predicted wt% spinel and the relative viscosity. Therefore, additional quenching experiments were conducted to identify the morphology and experimentally determined volume fraction of the spinel particles in the slag. These measurements revealed a difference in spinel size across the samples and corresponding viscosity behaviour, emphasizing the importance of spinel particle size on slag viscosity. Once the spinel size was taken into account, consistent viscosity results (relative apparent viscosity and flow index) were observed across the two devices. This study confirms that, once all parameters affecting slag viscosity are considered, the viscosity behaviour of a heterogeneous slag can be uniquely determined. The resulting optimized slag viscosity models can be used to predict viscosity before processing, addressing relevant phenomena such as slag tapping, slag foaming, and copper droplet settlement.

INTRODUCTION

Viscosity is one of the key physicochemical parameters to control during pyrometallurgical processes. Nowadays, a large amount of viscosity models are available to predict the viscosity of the liquid slag phase. However, the rheology of partially crystallised slags (a suspension, i.e. a liquid slag matrix with small solid particles suspended in the melt) remains insufficiently understood and a large discrepancy exists across various published works. (Sichen et al., 2022) Rheological aspects such as the non-Newtonian behaviour of slags containing suspended solid particles are poorly understood, resulting in a low reproducibility of the viscosity data across various studies. A key reason for the scatter on the obtained viscosity data is the lack of control / description of all parameters affecting the final viscosity of a heterogeneous slag. Liu et al., 2018 reviewed a large number of viscosity studies regarding heterogeneous silicate melts and reported the following parameters of interest: solid particle volume fraction, particle shape and the shear rate. For the particle shape, both the aspect ratio, i.e. the ratio of the longest axis of the particle to the shortest perpendicular axis, and the size were reported. In pyrometallurgical literature, the focus has mainly been on the aspect ratio of the particle as the main morphological parameter. (Liu et al., 2018)

Consequently, the main mode of shear thinning, i.e. the preferential re-orientation of the particles in the melt with respect to the flow direction, caused by a variation in the shear rate, was described in literature as individual particle orientation. This type of shear thinning has been visualised in FIG 1.A. Initially, the particles are randomly oriented. Upon shearing the suspension with an increasing flow rate, the hydrodynamic force acting on the particles increases, which causes the rotation of the particles around their axis perpendicular to the flow direction. Consequently, the flow lines of the melt are less disturbed, which causes a reduction in the apparent viscosity at large shear rates. Particles with a large aspect ratio can exhibit more of this type of shear thinning compared to equiaxed, symmetrical particles. (Mueller et al., 2009)

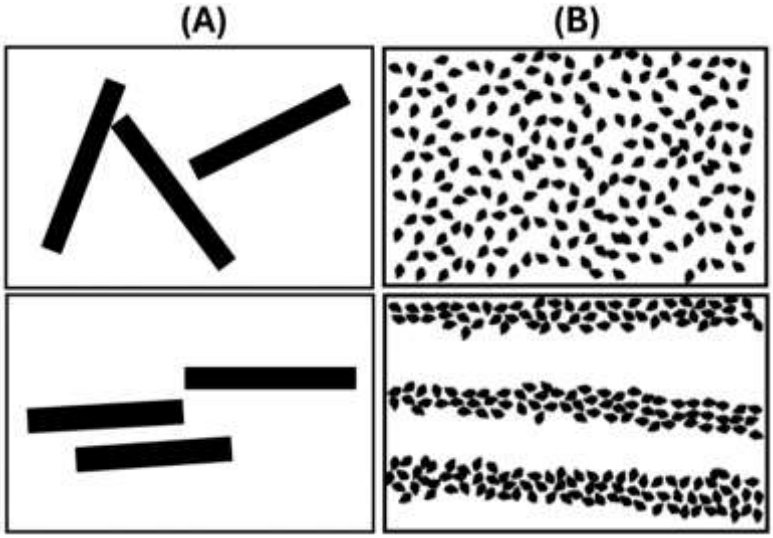

FIG 1 – Illustration of shear thinning, i.e. the re-orientation of the particles with respect to the flow direction. Top: random orientation, Bottom: preferential orientation with respect to the flow direction. **(A):** Individual particle orientation **(B):** Particle-particle orientation.

A second type of shear thinning is the particle-particle orientation, i.e. the re-orientation of the particles with respect to their closest neighbours. In FIG 1.B, at low shear rates and the associated random orientation of the particles, the path of the melt flow lines is largely disturbed. Upon shearing, the particles may group in more closely packed clusters to decrease the disturbance of the melt flow lines. (Carrchi et al., 2007) The elongated clusters have been observed experimentally by Lyon et al., 2001, for cold suspensions. Suspensions for which the suspended particles have a larger number of closest neighbours can exhibit this type of shear thinning to a larger extent. Consequently, the particle size will influence the degree of shear thinning associated with particle-particle orientation. Moreover, this mode of shear thinning also explains the observed shear thinning for suspensions containing spherical / equiaxed particles, which cannot show individual particle orientation. (Mueller et al., 2009, Saito et al., 2020)

For slag suspensions, literature commonly does not focus on the particle size. The work of Wright et al., 2000, is one of the few studies which examined the effect of the spinel size on the viscosity of a $CaO\text{-}MgO\text{-}Al_2O_3\text{-}SiO_2$ slag. Suspensions with three different spinel sizes were examined: 100-210 µm, 210-440 µm and 440-990 µm. They noted that the quality of their data was insufficient to make conclusions on the effect of particle size on the viscosity.

In our previous work (Vergote et al., 2023), the effect of the spinel size was examined for three different spinel sizes: small (13 µm), medium (34 µm) and large particles (76 µm). By employing a custom-built rheometer with quenching possibilities, accurate microscopical examination of the slag as it was during high-temperature viscosity measurement was possible. As a result, three accurate datasets were obtained from which the following conclusions were obtained:

1. The viscosity increases for decreasing spinel size at similar solid phase fractions.
2. Fully liquid samples at the spinel saturation composition showed Newtonian behaviour. Therefore, it is confirmed that no additional spinel particles located at the interface of the crucible and spindle (Vergote et al., 2021) affected the bulk slag viscosity measurement.

3. All examined samples containing spinel particles, even at low vol% of 1.8%, showed shear thinning behaviour. The amount of shear thinning increases for decreasing spinel size.

These conclusions were similar to the ones obtained from experiments with magmas containing solid particles. (Gaudio et al., 2013). Yet, additional viscosity data for slags relevant for the copper recycling industry are required to further establish the accuracy of our previous study. Therefore, this work examines the viscosity for slags with a relevant composition, while employing a different slag preparation and viscosity apparatus. This cross-check is required due to the low availability of accurate relevant viscosity data in literature, for which all parameters are well-described.

METHODOLOGY

Slag selection and preparation

An earlier work by the same authors identified the interaction between the slag and the alumina labware as the main experimental error for slag viscosity measurements. (Vergote et al., 2021). In this work, liquid lead-silicate based slag compositions were reported which were compatible with alumina, i.e. resulted in a low degree of interaction with crucible and spindle. One such composition (Slag 1, Table 1) was used in this work as the liquid slag matrix to prepare the heterogeneous slag-spinel samples. For this slag composition, it was confirmed that the interaction of the alumina spindle and crucible during the viscosity measurement is negligible. This slag is predicted by FactSage (Private database UQPY 2020) to be in equilibrium with spinel (with composition 'Spinel' in Table 1) at 1200°C. (Bale et al., 2016) A similar tie line approach as described in Vergote et al., 2023 was employed in this work. This approach includes a constant liquid viscosity of the slag matrix, with a composition fixed at the slag-spinel equilibrium, while uniquely varying the amount of spinel particles in the system across the various samples in the dataset. Therefore, the influence of the solid particles on the overall slag viscosity can be determined more accurately.

The 5 other bulk slag compositions (Slag 2-6, Table 1) were determined by adding the desired wt% equilibrium spinel composition to the liquid slag composition. All viscosity experiments were performed at 1200°C in order to maintain slag-spinel equilibrium and a constant liquid slag viscosity across the various samples.

TABLE 1 – Bulk slag and predicted spinel composition (wt%) for the considered samples for the slag-spinel suspensions. Slag liquidus temperature (T_{liq}) and the corresponding amount equilibrium weight fraction spinel (Sp.) particles at 1200°C were both calculated using FactSage (Private database UQPY 2020)

Sample	PbO	SiO_2	CaO	Al_2O_3	ZnO	Fe_2O_3	T_{liq} (°C)	Wt% Sp.
Slag 1	47.8	19.3	9.6	5.0	11.1	7.1	1200	0.0
Slag 2	46.8	18.9	9.4	4.9	11.6	8.2	1230	2.0
Slag 3	45.9	18.5	9.2	4.9	11.9	9.3	1258	3.8
Slag 4	44.8	18.1	9.0	4.8	12.5	10.7	1279	6.2
Slag 5	43.8	17.5	8.7	4.7	13.1	12.6	1321	9.4
Slag 6	40.5	16.3	8.1	4.5	14.4	16.0	1371	15.2
Spinel	0	0	0	1.5	32.5	66.0	/	100.0

All samples were pre-melted using an induction furnace (Hüttinger TIG 20/100) using the methodology described earlier in (Vergote et al., 2021). First, at 1200°C, the slag subsystem (PbO-SiO_2-CaO-Al_2O_3-ZnO) was pre-melted for one hour. FactSage predictions indicated that for all samples, these slag subsystems were fully liquid at this temperature. As a result, low viscosity samples were obtained which enhanced mixing and melting of all powder chemicals. After the pre-melting, the required amount of Fe_2O_3 powder was added to the crucible. This resulted for slag samples 2-6 in the precipitation of spinel particles in the slag, where the Fe_2O_3 acted as a nucleating agent for these particles. The slag was further homogenised and mixed by blowing air in the bath

through an alumina blowing tube for one hour to ensure homogeneity of the sample. Afterwards, the slag was quenched in water. Microscopical analysis indicated proper dissolution of all chemicals and formation of spinel particles, i.e. no large Fe_2O_3 powder particles but all well-formed crystalline spinel particles. The obtained slag particles were used as starting material for the viscosity measurements.

Viscosity measurements

Viscosity measurements were performed using a Searle concentric cylinder set-up in an Anton Paar FRS 1800 rheometer, consisting of an alumina spindle and crucible. The details of this apparatus were described previously in (Vergote et al., 2021). The necessary amount of slag (± 150 g) was determined based on the slag density to yield a 9 mm slag layer above and below the spindle, in order to minimise the effect of the spindle height on the obtained viscosity values (Chen et al., 2013). The quenched slag particles from the pre-melting were directly heated to 1200°C at a heating rate of 5°C/min. Subsequently, the slag was homogenised for one hour in order to obtain thermal and chemical equilibrium. Afterwards, the spindle was inserted into the slag bath and the measurement sequency as described before (Vergote et al., 2021) was executed. Fully liquid slag samples behave Newtonian, i.e. the viscosity is independent of the shear rate, whereas slag samples containing solid particles show shear thinning behaviour, i.e. a decreasing viscosity with increasing shear rate. Therefore, it is necessary for slag samples containing solid particles to examine the viscosity at various shear rates ($\dot{\gamma}$ = 0.245 – 24.5 s^{-1}) to get a comprehensive understanding of the rheological behaviour of the sample. Once the measurements were finished, the slag was slowly cooled (5°C/min) to room temperature.

Several repetition viscosity experiments were performed in order to verify the consistency of the obtained results. For each experiment, a unique slag batch was prepared using the methodology described above.

To enable the comparison of the obtained viscosity dataset with the previous viscosity data, the apparent viscosity data, i.e. measured at a specific shear rate, is converted to the apparent relative viscosity (η_{rel}):

$$\eta_{rel} = \frac{\eta_{app}}{\eta_{liq}}$$

With η_{app} the apparent viscosity and η_{liq} the viscosity of the liquid slag matrix. As a result, the effect of solid particles in suspensions on the overall viscosity can be examined across heterogeneous slag samples with a different liquid slag viscosity.

Quenching experiments & microscopical analysis

In contrast to custom-built rheometer from the previous work (Vergote et al, 2023), it is not possible to quench samples directly after viscosity measurement in the FRS 1800. Quenching experiments were performed using the slowly cooled slag from the viscosity measurement. Slag particles in between the spindle and crucible (i.e. the measurement gap) were removed from the sample. These particles were used as the material for the quenching experiment to examine the microstructure of the sample as it was at high-temperature. 20 g of slag was added to an alumina crucible which was suspended in the hot zone of a resistance tube furnace (Carbolite HTRV 1800). The sample was heated from room temperature at a heating rate of 5°C/min and held for one hour at 1200°C. Afterwards, the wire suspending the crucible was cut from above and the sample was rapidly quenched in a water bucket. The quenched crucible was cross-sectioned, cold embedded in Epofix resin and prepared for microscopical analysis.

The microstructure of the samples was examined using a scanning electron microscope (SEM, JEOL, JSM-7600, FEG-SEM). The SEM was operated in backscattered electron (BSE) mode to increase the contrast between the amorphous slag phase and the spinel particles. The volume fraction, size and aspect ratio of the spinel particles was determined using ImageJ. These parameters were determined using at least 20 SEM-BSE images randomly selected in the bulk of the quenched sample. For the size of the particles, the Sauter average diameter is reported, since this parameter was found to be more suitable to describe the rheology of slag suspensions. (Vergote et al., 2023). It is defined as:

$$D_{sauter} = \frac{\sum_{i=1}^{n} D_i^3}{\sum_{i=1}^{n} D_i^2}$$

With D_{sauter} the Sauter average diameter, D_i the diameter of the spinel particles of a certain particle 'i' and n the amount of considered spinel particles.

RESULTS & DISCUSSION

This study

Slag 1 showed a Newtonian flow behaviour with a constant viscosity of 0.45 Pa.s over the entire shear rate range ($\dot{\gamma}$ = 0.245 – 24.5 s^{-1}). This viscosity was used to determine the relative viscosity for the other samples within this dataset. All other samples showed shear thinning behaviour, therefore it is required to define the shear rate to report the apparent viscosity. FIG 2.a shows the relative viscosity increase for the calculated spinel weight fractions (Table 1) for the various samples at $\dot{\gamma}$ = 24.5 s^{-1}. First of all, a large scatter on the relative viscosity can be seen for the repetition experiments of slags 3, 4, 5, e.g. both η_{rel} = 1.8 and 7.1 were measured for the similar intended slag composition slag 5.

As discussed in the introduction, there is a large number of parameters which affect the overall viscosity of a heterogeneous slag. Since every experiment in FIG 2.a originates from an individual pre-melt, the consistency of the morphology of the spinel particles is not guaranteed. Therefore, additional quenching experiments were performed on selected samples (purple markers in FIG 2.a) in order to determine the volume fraction of the spinel particles and their morphology.

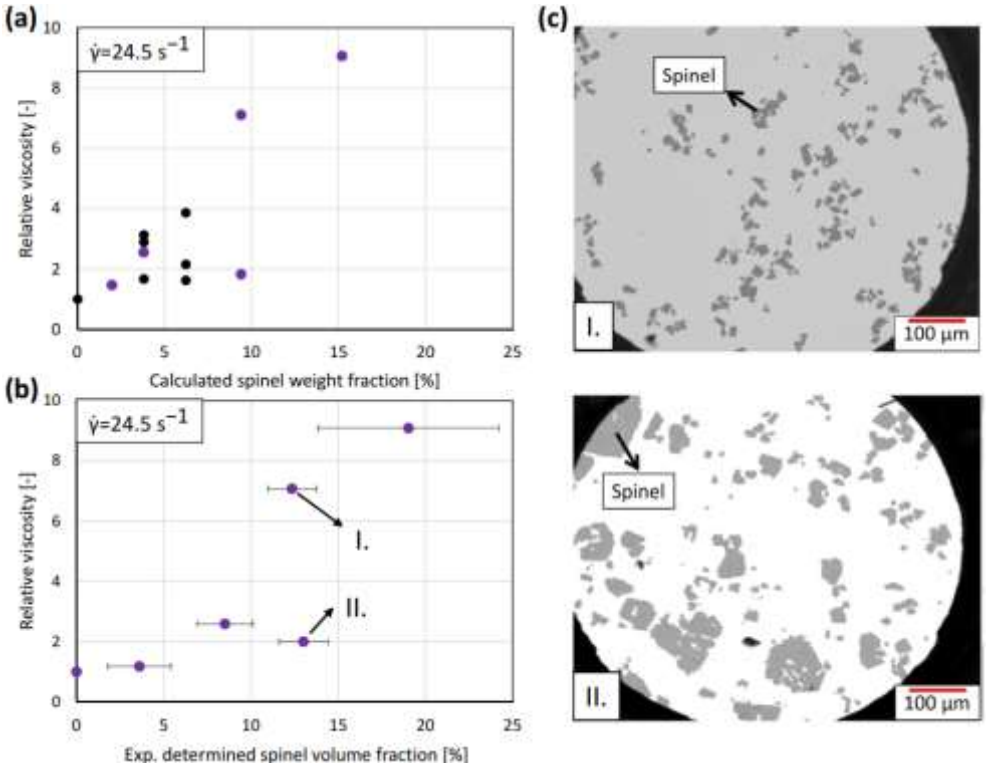

FIG 2 – **(a):** Relative viscosity (η_{liq}= 0.45 Pa.s, 1200°C) at $\dot{\gamma}$ = 24.5 s^{-1} for all samples in this dataset, as a function of the calculated spinel weight fraction (Table 1). The purple markers indicate the samples for which additional quenching experiments were performed. **(b):** Relative viscosity at $\dot{\gamma}$ = 24.5 s^{-1} of the selected samples from (a), for which the volume fraction was experimentally determined. **(c):** SEM-BSE images of samples I and II from (b)

FIG 2.b shows the relative viscosity as a function of the experimentally determined spinel volume fraction for a selected number of samples. A first conclusion is that the volume fraction is higher for each sample compared to the predicted weight fraction, caused by the density difference between the slag and spinel particles (Vergote et al., 2023). This observation highlights the importance of experimentally determined parameters instead of thermodynamic predictions to examine the

rheological behaviour of slag samples. Moreover, quenching experiments were performed on the two repetition experiments of slag 5 (9.4 wt% spinel). For the two samples, a similar volume percentage of spinel particles was present in the slag, i.e. 12.4 and 13.0 vol% spinel. Therefore it can be concluded that the reproducibility of the pre-melting step is high. Yet, despite their similar volume percentage, a significantly different relative viscosity was obtained at $\dot{\gamma}$ = 24.5 s^{-1}. The microstructures of both repetition experiments of slag 5 (I and II) are shown in FIG 1.c. First, the aspect ratio of all spinel particles was constant (± 1.5) for all observed quenched samples. Second, the spinel particles for sample II are significantly larger (D_{sauter} = 78 µm) compared to the spinel particles of sample I (D_{sauter} = 30.2 µm). It was concluded before that large spinel particles cause a lower viscosity increase compared to small particles. (Vergote et al., 2023) Lastly, the microstructures of the other samples which were microscopically studied (Slags 2,3,6) showed spinel particles with a size similar to sample I.

In the previous study, the size of the spinel particles was controlled by pre-sintering the spinel particles before adding them to the liquid melt. In this work, Fe_2O_3 powder was added to the liquid PbO-SiO_2-CaO-Al_2O_3-ZnO slag subsystem at 1200°C. This powder acted as a heterogeneous nucleating site for spinel particles. Using this methodology, the spinel size is largely affected by the Fe_2O_3 powder size and possible agglomeration of powder upon adding it to the liquid slag. Therefore, using this methodology, there is no control over the spinel size. The lack of control over this parameter, which is known to largely affect the slag viscosity, results in the observed scatter in FIG 2.a and 2.b for a constant intended amount of spinel particles.

Comparison to the previously obtained datasets

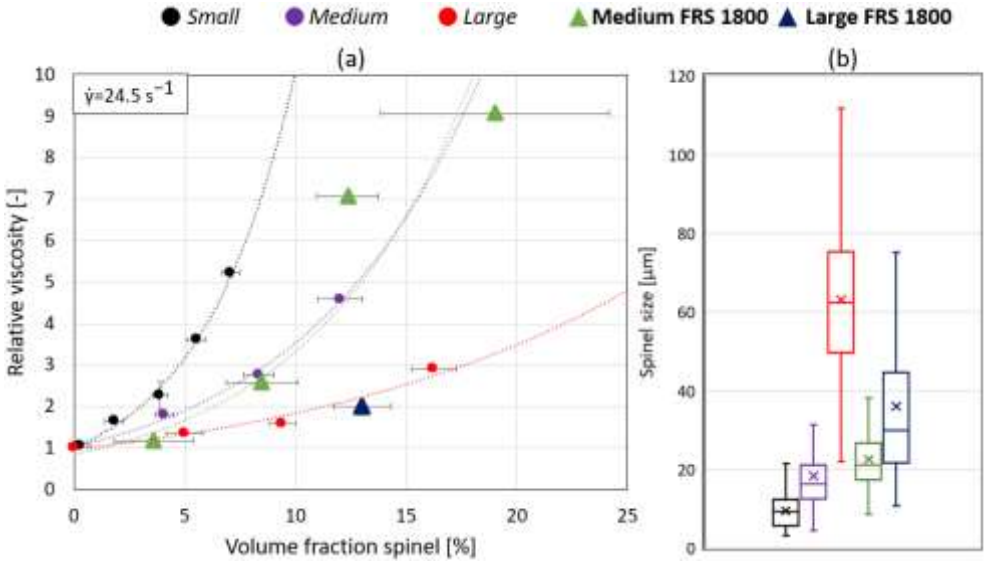

FIG 3 – **(a):** Comparison of the relative viscosity at $\dot{\gamma}$ = 24.5 s^{-1} for the samples in this work (triangles, medium and large FRS 1800) and the ones from the previous work (circles, small, medium and large, Vergote et al., 2023). The dotted lines represent optimisations of the Krieger-Dougherty equation for each dataset. **(b):** Spinel particle size boxplots for all considered datasets, the number-average diameter is indicated with a x-marker on each boxplot.

From the discussion above, it is clear that for the samples for which the volume fraction was experimentally determined, all samples except repetition experiment II from slag 5 had an equal spinel size. Therefore, the dataset in this work is divided in two sub datasets, the samples with a medium spinel size (Medium FRS 1800) and the one sample of slag 5 with the large spinel particles (Large FRS 1800). These two datasets can be compared with the three previously obtained datasets from (Vergote et al., 2023), where the spinel particle size was well-controlled. FIG 3.b shows the distribution of the spinel particle size for the 5 datasets, the small, medium and large dataset from the previous work (Vergote et al., 2023) and the medium and large FRS 1800 dataset from this work. It is important to note that not only the number average spinel diameter should be considered (x-markers on FIG 3.b) to define the size of the particles in a dataset, but the entire distribution. The boxplots of the two medium datasets agree well and therefore their viscosity results can be compared against each other. The number average of the large FRS 1800 dataset (36 µm) is significantly

smaller compared to the previously obtained dataset with large spinel particles (62 µm). Yet, based on their Sauter-average diameter, 61 and 78 µm for the FRS and the previous dataset, respectively, the difference between both datasets is smaller, due to several large spinel particles in the FRS dataset, seen by the large upper limit of the boxplot.

The spinel volume fraction - relative viscosity trend at $\dot{\gamma}$ = 24.5 s^{-1}, reported in FIG 3.a, agrees well for both medium datasets. In the previous dataset, the maximal volume fraction was limited to 12.0 vol% whereas in the FRS 1800 this is extended to 19.2 vol%. To all datasets, Krieger-Dougherty equations were fitted to correlate the relative viscosity with the solid volume fraction. (Krieger & Dougherty, 1959) The trend from the medium FRS 1800 datasets agrees well with the extrapolated trend from the previous dataset. The one datapoint from the large FRS 1800 dataset corresponds with the trend of the large dataset from the previous study, despite the slightly smaller spinel particles in the FRS 1800 dataset.

A second parameter to be able to compare the rheological behaviour across various datasets is the flow index. This parameter is fitted to the flow curves and reflects the degree of shear thinning (n = 1 reflects Newtonian behaviour, n < 1 reflects shear thinning behaviour). An Ostwald-de Waele equation is fitted to the flow curves:

$$\eta_{app} = K * \dot{\gamma}^{n-1}$$

Where K is a parameter which equals the viscosity at $\dot{\gamma}$ = 1 s^{-1} and n is the flow index, respectively. Similar to the previous work, the shear rate range 2.4 – 10 s^{-1} was considered in order to avoid the second Newtonian regime at large shear rates (Vergote et al., 2023). The resulting flow indices for various volume fractions are shown in FIG 4. First of all, all datasets show a decreasing flow index, i.e. more shear thinning, with increasing volume fraction of spinel particles. This observation can be explained by the increased number of particles with increasing volume fraction. As a result, the particles have more close neighbours in the melt to be influenced by (particle-particle orientation) and consequently the internal structure can be more affected by the shear rate. (Vergote et al., 2023) Secondly, the large FRS 1800 dataset show less shear thinning compared to the medium dataset. This observation can be explained in a similar way: a decrease in particle size, for a constant volume fraction, result in a larger number of particles, hence more particle-particle orientation. Both rheological observations, a smaller relative viscosity (FIG 3.a) and the lower degree of shear thinning, can be explained by the microstructural observation of the larger spinel particles.

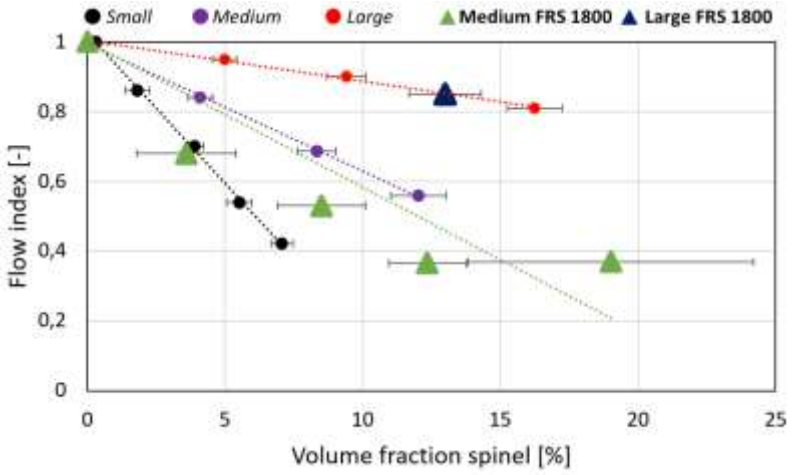

FIG 4 – Flow index as a function of the experimentally determined spinel volume fraction for all considered datasets. Linear trendlines (dotted lines) were fitted to all datasets.

Moreover, the flow indices of the medium FRS dataset from this work are slightly smaller compared to previously obtained flow indices for the medium dataset. Furthermore, it is observed that the flow index does not further decrease at larger spinel volume fractions. This flow index plateau is also commonly reported in literature. (Mueller et al., 2009) Therefore, the applicability of the linear trendline may be limited at large volume fractions. For the large FRS dataset, the flow index aligns with the previously determined trendline for the large spinel particles, despite the small difference in size between both datasets (FIG 3.b).

CONCLUSION

The previous study largely focused on providing reliable datasets with a strong control over all parameters affecting the rheology of heterogeneous slag containing spinel particles. The methodology involved control over the spinel particle size via pre-sintering the spinel particles before adding them to the liquid melt. This study was performed to verify the consistency of the previously obtained insights in the viscosity behaviour of a slag containing spinel particles.

In this study's methodology, the size of the spinel particles was not well-controlled, which was reflected in the scatter on the relative viscosity for a constant intended amount of spinel particles. Microstructural analysis of quenched samples showed that the spinel size differed across various samples. Therefore, the samples were divided into two datasets, with medium and large spinel particles. Similar to the conclusions from the previous study, it was observed that the relative viscosity increase was larger for smaller spinel particles. Moreover, the samples with smaller spinel particles also showed stronger shear thinning behaviour, which was also previously concluded. The numerical values for the relative viscosity and the flow index were in the similar range as the one determined earlier.

This study further supports the importance of considering the particle size for viscosity studies and models regarding heterogeneous silicate melts. As a result, particle-particle orientation as a mode of shear thinning should also be considered. The initially obtained conclusions are further supported by this study, using an independent slag preparation and different high-temperature rheometer.

ACKNOWLEDGEMENTS

O. Vergote holds a grant (No. HBC.2023.0671) which is supported by VLAIO, the Flanders Innovation & Entrepreneurship Agency, in co-operation with Umicore. I. Bellemans holds a grant from the Research Foundation Flanders (No. 1239024N)).

REFERENCES

C. W. Bale, E. Bélisle, P. Chartrand, S. A. Decterov, G. Eriksson, A.E. Gheribi, K. Hack, I. H. Jung, Y. B. Kang, J. Melançon, A. D. Pelton, S. Petersen, C. Robelin. J. Sangster, P. Spencer and M-A. Van Ende, FactSage Thermochemical Software and Databases - 2010 - 2016, Calphad, vol. 54, pp 35-53, 2016

Caricchi, L.& Burlini, L. & Ulmer, P. & Gerya, T. & Vassalli, M. & Papale, P. (2007). Non-Newtonian rheology of crystal-bearing magmas and implications for magma ascent dynamics. Earth and Planetary Science Letters. 264. 402-419.

Chen, M. & Zhao, B. (2015). Viscosity Measurements of SiO2-"FeO"-CaO System in Equilibrium with Metallic Fe. Metallurgical and Materials Transactions B. 46. 577-584.

Del Gaudio, P. & Guido, V. & Taddeucci, J. (2013). The effect of particle size on the rheology of liquid-solid mixtures with application to lava flows: Results from analogue experiments: Rheology of Liquid-Solid Mixtures. Geochemistry Geophysics Geosystems 14(8):2661–2669.

Krieger, IM, Dougherty, TJ (1959) A mechanism for non-Newtonian flow in suspensions of rigid spheres. Transactions of the Society of Rheology 3: 137–152.

Lyon, M.K., Mead, D.W., Elliott, R.E., Lea, L.G. Structure formation in moderately concentrated viscoelastic suspensions in simple shear flow. J. Rheol. 1 July 2001; 45 (4): 881–890.

Liu, Z. & Pandelaers, L. & Blanpain, B. & Guo, M. (2017). Viscosity of Heterogeneous Silicate Melts: Assessment of the Measured Data and Modelling. ISIJ International. 57. 1895-1901.

Mueller, S. & Llewellin, E. & Mader, H.. (2009). The rheology of suspensions of solid particles. Proc. R. Soc. A Proc. R. Soc. A. 466. 1201-1228.

Saito, N. & Hara, D. & Teruya, S. & Nakashima, K. (2020). Viscosity of Slag Suspensions with a Polar Liquid Matrix. ISIJ International. 60. 2807-2818.

Sichen, D., Huss, J., Vickerfält, A., Berg, M., Martinsson, J., Allertz, C. and Kojola, N. (2022), The Laboratory Study of Metallurgical Slags and the Reality. steel research int., 93: 2100132.

Vergote, O. & Bellemans, I. & Van den Bulck, A. & Verbeken, K. (2021). Towards More Reliable PbO-SiO2 Based Slag Viscosity Measurements in Alumina via a Dense Intermediate Spinel Layer. Metallurgical and Materials Transactions B *52*(6), 3646–3659.

Vergote, O. & Bellemans, I. & Van den Bulck, A. & Shevchenko, M. & Starykh, R. & Jak, E. & Verbeken, K. Viscosity experiments of slag-spinel suspensions: The effect of volume fraction, particle size, and shear rate. *J. Rheol.* 1 November 2023; 67 (6): 1159–1174.

Wright, S. & Zhang, L. & Sun, S. & Jahanshahi, S. (2000). Viscosity of a CaO-MgO-Al2O3-SiO2 melt containing spinel particles at 1646K. Metallurgical and Materials Transactions B 31. 97-104.